Chapter 4

Distribution of sojourn times for wave reflection from a random potential

4.1 Introduction

When a wavepacket centered at an energy E is scattered elastically from a scattering potential, it suffers a time delay before spreading out dispersively. This delay is related to the time of sojourn of the wave in the interaction region. Thus scattering delay time is the single most important quantity describing the time-dependent aspect i.e., physically, the reactive aspect of the scattering in open quantum systems, *e.g.* the chaotic microwave cavity and the quantum billiard (whose classical motion is chaotic) and the solid-state mesoscopic dots coupled capacitively to open leads terminated in the reservoir. The delay time is described well in many situation by the energy(E) derivative of the phase shift (ϕ) suffered in the scattering, $\hbar(\partial\phi/\partial E)$, first introduced by Wigner [69]. This was later generalized to the case of a scatterer coupled to N open channels leading to the continuum, where one defines the phase shift time delays through the Hermitian energy derivative of the S-matrix, $-i\hbar S^{-1}\partial S/\partial E$, the average of whose eigenvalues gives the Wigner-Smith delay times [112]. This aspect of time delay associated with waves scattered by disordered media has assumed importance in view of the recent measurements carried out in disordered waveguides for microwaves [113] and mesoscopic systems. In fact,the delay time can be used as a diagnostic tool[114, 115] for localization of light [44]. The static signature of localization, an exponential decay of the transmitted intensity with sample thickness, is non-unique since absorption can also give an exponential decay. This reason is at the heart of the

controversy regarding the experimental demonstration of localization of light in three dimensions [45]. Localization and absorption would, however, give entirely different dynamical behaviour of the time delay of scattering. The delay time is, however, not self averaging and one must have its full probability distribution over a statistical ensemble of random samples.

The distribution of these delay times for a wave reflected/transmitted from/through a random medium has been a matter of intense research in recent years [116, 106, 117, 118, 119, 120, 121, 122, 123, 107, 114, 124]. The distribution may be related ergodically to the ensembles generated parametrically, *e.g.*, by energy E variation over a sufficient interval. Thus we have the random matrix theory (RMT) for circular ensembles of the S-matrix giving delay times for all the three Dyson Universality classes for the case of a chaotic cavity connected to a single open channel [125]. Generalization to the case of N channels corresponded to the Laguerre ensemble [126] of RMT. The RMT approach has been treated earlier through the supersymmetric technique for the case of a quantum chaotic cavity having a few equivalent open channels [127]. However it has been suspected for quite sometime that the RMT based results and the universality claimed thereby may not extend to a strictly 1-dimensional random system where Anderson localization dominates, and that the 1D random system may constitute after all a different universality class [128]. This important problem has been re-examined recently by Texier and Comtet [116] who have derived the delay time distribution for a 1D conductor with the Frish-Lloyd model of randomness, in the limit of high energy / weak disorder and the sample length $\gg$ the localization length. The universality of the distribution is amply supported by numerical simulations for different models of disorder [116, 120].

In this work, we re-examine this question of universality of the delay time distribution for a 1D random system and relate it to the universality of distribution of the reflection coefficient, a quantity that we have direct access to from the earlier work [55]. To this end, we will calculate the distribution of the literal sojourn times for a 1-D(one-channel) random potential using the 'Non-Unitary' clock discussed in Chapter-3. This involves adding an infinitesimally small but spatially uniform imaginary potential iV_i to the 1-D random potential V_r.[1] This obviates the need to

[1] As shown in Chapter-3, the effects of the 'spurious' scatterings associated with mismatch due to the imaginary potential are expected to cancel out for a random potential and we do not need

calculate the energy derivative of the phase to obtain the Wigner delay time and its distribution [117]. We derive probability distribution of the reflection sojourn times in the weak disorder/high energy limit. The distribution derived by us agrees exactly with the universal Wigner delay time distribution of Texier and Comtet [116]. Besides, our new technique allows us to treat the sojourn time distribution for the important case of light reflected from a random amplifying medium equally well. In this case however, unlike the case for the passive random medium, all moments of the delay time are finite for long samples. We then re-examine an earlier calculation of the Wigner delay time distribution [117, 119] using the method of invariant imbedding, where a slightly different expression was reported. We find that the difference arises due to the inconsistency of the approximations involved within the random phase approximation (RPA) and find that when the approximations are carried out consistently, their expression reduces to ours.

We will then examine numerically, the distribution of delay times for strong disorder using the transfer matrix method for a one-dimensional disordered chain with a one-band tight binding Hamiltonian. We find that the distribution of Wigner phase delay times and the sojourn times clocked by the non-Unitary clock agree exactly even in the strong disorder regime for energies far away from a band-edge. We further examine the effect of a periodic background on the delay time by varying the energy within the band. We find that, for energies close to a band-edge and strong disorder, the Wigner delay time distribution differs considerably from that of the sojourn time given by the Non-Unitary clock. The Wigner delay time can even become negative under such conditions. The sojourn time, however, remains positive.

4.2 The sojourn time for wave reflection from a random potential

Consider first the electronic case for a 1D disordered sample of length L having a random potential V_r , $0 \leq \mathrm{x} \leq \mathrm{L}$, and connected to infinitely long perfect leads at the two ends. Let the electron wave of energy $\mathrm{E} = \hbar^2 k^2/2m$ be incident from the right at $\mathrm{x} = \mathrm{L}$, and be partially reflected with a complex amplitude reflection coefficient

to correct for these. Further, for the case of total reflection $|R| \simeq 1$, the dwell time is literally given by this quantity and also it is related to the Wigner phase delay time.

$R(L) = |R(L)| \exp[i\theta(L)]$ and $|R(L)|^2 = r(\mathrm{L})$, the real reflection coefficient. Inside the sample we have the Schrodinger equation,

$$\frac{d^2\psi(x)}{dx^2} + k^2 [1 + \eta_r(x)]\, \psi(x) = 0, \tag{4.1}$$

with $\eta_r(x) = -V_r(x)/E$.

As we will be interested in the reflection coefficient, it is apt to follow the invariant imbedding technique [55, 117, 96, 129, 97] (see Appendix-A) and reduce the Schrodinger equation(4.1) to an equation for the emergent quantity $R(L)$:

$$\frac{dR(L)}{dL} = 2ikR(L) + \frac{ik}{2}\eta_r(L)\,[1 + R(L)]^2 \tag{4.2}$$

We now introduce a uniform imaginary part iV_i, with $V_i > 0$, and accordingly define $\eta(L) = \eta_r + i\eta_i$, with $\eta_i = -V_i/E$. For analytical treatment, we take for $V_r(x)$ a Gaussian delta-correlated random potential (the Halperin model) with $< \eta_r(L) >= 0$ and $< \eta_r(L)\eta_r(L') >= \mathrm{A^2S(L - L')}$. The Fokker-Planck equation corresponding to the stochastic equation(4.2) can be solved analytically in the limit $\mathrm{L} \to \infty$ giving [55]:

$$\begin{aligned} P_\infty(r) &= \frac{D \exp\left(-\frac{D}{r-1}\right)}{(r-1)^2} \quad , \qquad r \geq 1 \\ &= 0 \qquad\qquad\qquad\quad , \qquad r < 1 \end{aligned} \tag{4.3}$$

with $\mathrm{D} = (8\mathrm{V},)/(\mathrm{EA^2k})$. This result is obtained in the high energy / weak disorder limit. The result for an absorbing medium ($V_i < 0$) can be similiarly written as

$$\begin{aligned} P_\infty(r) &= \frac{|D| \exp(|D|) \exp\left(-\frac{|D|}{1-r}\right)}{(1-r)^2} \quad , \qquad r \leq 1 \\ &= 0 \qquad\qquad\qquad\qquad\quad , \qquad r > 1. \end{aligned} \tag{4.4}$$

4.2.1 The case of a passive random medium

Now, clearly for a passive medium, *i.e.*, with $V_i = 0$, the distribution $P_\infty(r)$ must collapse to a delta-function $\mathrm{S(r - 1)}$ as $\mathrm{L} \to \infty$. However, with $V_i \neq 0$, for a short sojourn time T in the sample, the reflection coefficient $r = |R|^2 = \exp(2V_iT/\hbar)$, giving $r - 1 = 2V_iT/\hbar$ to first order in V_i as V_i is taken to be arbitrarily small. Thus, $P_\infty(r)$ can at once be translated into the sojourn time distribution $P^0_\infty(\mathrm{r})$:

$$P^0_\infty(\mathrm{r}) = \frac{\alpha}{\mathrm{r}} \exp\left(-\frac{\alpha}{\tau}\right), \tag{4.5}$$

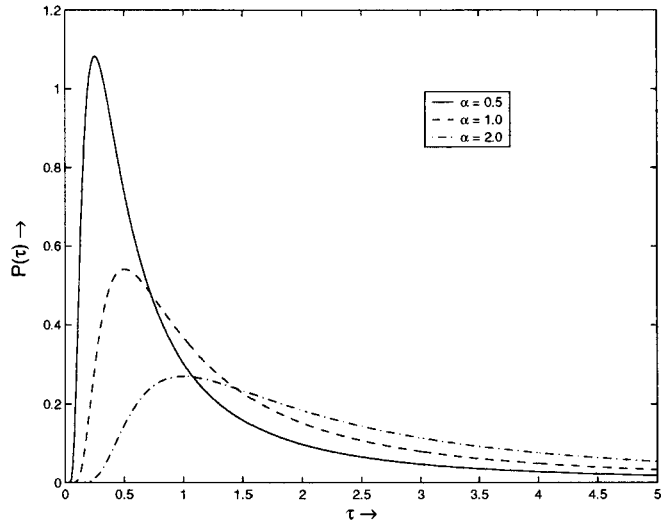

Figure 4.1: The delay time distribution from a long disordered passive medium.

where $a = 4(\Delta^2 k)^{-1}$ and the dimensionless time $\tau = ET/\hbar$. This is precisely the result of Texier and Comtet [116]. Note that V_i, the counter, drops out in the limit $V_i \to 0$, as it should.

We show the distribution of the sojourn times in Fig. (4.1) for different values of the parameter a. The distribution has a maximum value at $\tau_{max} = 0.5\alpha$ and a τ^{-2} tail for large τ ($\tau \to \infty$) giving a logarithmic divergence of the average sojourn time. In fact, all the moments of this distribution $P^0_\infty(\tau)$ are infinite. The counter introduced by us literally counts the time of sojourn in the interaction region for total reflection in the ID, *i.e.*,1-channel case. Large delay time is dominated by the dwell time when the wave penetrates deeper into the sample, which is true at high energy/low disorder. It is this 'equilibrated' part of the reflected wave, and not the prompt part that is expected to give universality. Hence the universal $1/\tau^2$ tail in equation(4.5). Indeed, the universality of the delay-time distribution directly reflects that of the reflection coefficient given by equation(4.3) [57, 58, 63]. Indeed, we have verified that Eqn.(4.3) is obtained for telegraph disorder also (see Chapter-2). The logarithmic divergence of the average sojourn time indicates the possibility of the particle traversing the entire (infinite) length of the sample before being reflected and is a manifestation (as indicated in [117]) of the log-normal distribution of the conductance in the localized regime caused by Azbel resonances [130]. It is to be

remarked here that this universal delay time distribution as in equation(4.5), is not obtained for a chaotic cavity connected to a reservoir by a single open channel [125]. Here the localization picture may not hold.

4.2.2 The case of an active random medium

Encouraged by this result for for the electronic case, we now turn to the case of a light wave reflected from a random amplifying medium (RAM). The latter is recieving much attention in recent years in the context of random lasers [16, 86, 54]. To fix ideas, consider the case of a single mode optical fibre doped with Er^{3+}, say, optically pumped and intentionally disordered refractively. For the case of light, $\eta(L) = \eta_r(L) + i\eta_i$ corresponds to the refractive index of the medium with the real part varying in space, while the imaginary part η_i which causes absorption/amplification is spatially constant. All we have to do now is to keep V_i finite, a measure of medium gain, and use $\mathrm{T} = (\hbar/2)\ (\partial \ln r/\partial V_i)$ for the sojourn time, and translate $P_\infty(r)$ into $P_\infty(\tau)$:

$$P_\infty(\tau) = (D\xi)\frac{\exp\left(-\frac{D}{e^{\xi\tau}-1}\right)}{(e^{\xi\tau}-1)^2}e^{\xi\tau}, \tag{4.6}$$

where $\xi = 2V_i/E$. Again, P_∞ vanishes in the limit $\tau \to \infty$ as also for $\tau \to 0$. Also, $P_\infty(\tau) \to P_\infty^0$ as $V_i \to 0$. All moments $< \tau^n >$ are however finite in this case. An explicit expression can be obtained for the first moment as :

$$\langle\tau\rangle = \frac{\mathrm{I}}{\xi}\left[\ln \mathrm{D} + C - e^D Ei(-D)\right], \tag{4.7}$$

where C is the Euler's constant [131] and Ei is the exponential integral [131]. This expression diverges as $V_i \to 0$. In Fig. 4.2, we show the delay time distributions given by Eqn.(4.6) for different values of the parameter ξ, while keeping a fixed, corresponding to different values of the imaginary potential V_i while keeping the disorder fixed.

Some interesting points are to be noted here. First we note that the distribution of sojourn times for an absorbing medium is the same as that for an amplifying medium. This is due to the well-known symmetry between absorption and amplification [94]. The finiteness of the moments in the case of an absorbing medium is easily understood in that the longer paths are attenuated by absorption. In the case of the random amplifying medium, the effect is more subtle. The finiteness of all the moments is

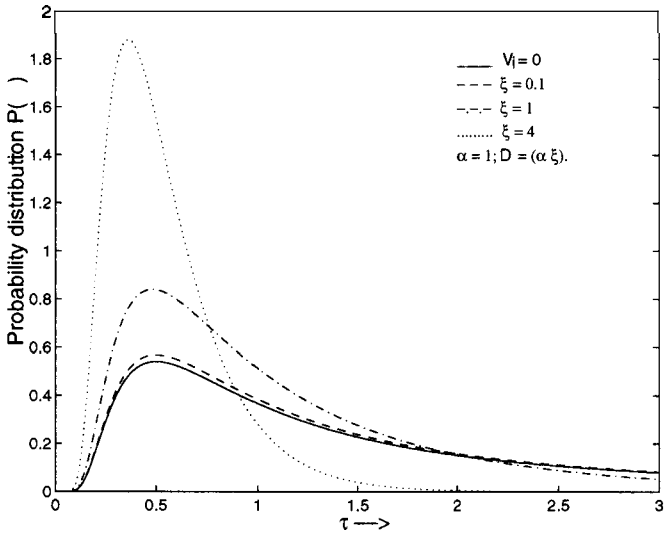

Figure 4.2: The delay time distribution from an amplifying medium.

essentially due to the well known fact that amplification enhances localization and prevents deep penetration in the medium. Of course, there is also an enhanced prompt part of reflection resulting from the increased refractive index mismatch in respect of its imaginary part at the sample-lead interface.

4.3 Distribution of Wigner delay time for reflection

Here we will reconsider the earlier calculation of Jayannavar et al. [117, 119] for the distribution of the Wigner phase delay time for total reflection from a one-dimensional (one-channel) disordered medium. Again, we will begin with the invariant imbedding equation for the reflection amplitude $R(L) = \sqrt{r(\mathrm{L})}\exp[i\theta(L)]$ given by Eqn.(4.2). In the limit of large lengths (L $\gg l_c$, the localization length), the reflection becomes approximately unitary $r(L) \simeq 1$ and Eqn.(4.2) yields an equation for the phase $\theta(L)$ as

$$\frac{d\theta}{dL} = 2\mathrm{k} + k\eta_r(L)(1 + \cos 0) \tag{4.8}$$

The equation for the phase delay time $T_\phi = \hbar(d\theta/dE) = 1/c_g(d\theta/dk)$ (where c_g is the group velocity), is obtained by differentiating the above equation for 0 with respect

to k:

$$\frac{dT_\phi}{dL} = \frac{1}{c_g}\left[2 + \eta_r(L)\,(1 + \cos\theta - kc_gT_\phi \sin\theta)\right]. \tag{4.9}$$

As before, we will assume that the random refractive index $\eta_r(L)$ to be a Gaussian white noise with a zero mean, i.e., $\langle \eta_R(L)\rangle = 0$ and $\langle \eta_R(L)\eta_r(L')\rangle = \mathrm{A}^2 6(\mathrm{L} - \mathrm{L}')$. Using the Novikov theorem [100] (see Appendix-B), we can now set up a Fokker-Planck equation for the joint probability distribution function $P(T_\phi, \theta; \mathrm{L})$ over the ensemble of $\eta_r(L)$. However, we will be interested in the marginal probability distribution $P(T_\phi; \mathrm{L})$ alone, which can be obtained by integrating over the phase angle θ. To this end, we make the random phase approximation (RPA) and set $P(T_\phi, \theta; \mathrm{L}) = P(T_\phi; L)/2\pi$, i.e., assume a uniform distribution over the phase angle θ. The RPA is a good approximation at high energies and weak disorder. We obtain the equation for $P(T_\phi; \mathrm{L})$ as

$$\frac{\partial P}{\partial l} = \frac{\partial}{\partial T_\phi}\left[\frac{\partial}{\partial T_\phi}\left(\frac{T_\phi^2}{2} + \frac{3}{2c_g^2k^2}\right) + \left(T_\phi - \frac{4}{c_g\Delta^2k^2}\right)\right] P, \tag{4.10}$$

where the dimensionless length $l = L/l_c = 1/2\ \mathrm{A}^2\mathrm{k}^2\mathrm{L}$. In the limit of large lengths, $1 \gg 1$, the distribution saturates and we can set $\partial P/\partial l = 0$. Hence, we obtain the solution

$$P_\infty(\tau) = \frac{\lambda e^{\lambda \tan^{-1}\tau}}{(e^{\lambda\pi/2} - 1)(1 + \tau^2)} \tag{4.11}$$

where $\lambda = 8/\sqrt{3}\Delta^2 k$ and the dimensionless time $\tau = c_g k T_\phi/\sqrt{3}$. This expression also yields a τ^{-2} behaviour for $\tau \to \infty$, but differs from the universal distribution of sojourn imes given by Eqn.(4.5). The main difference appears at $\tau = 0$, where this expression for $P_\infty(\tau)$ yields a finite value in contrast to Eqn.(4.5), which gives $P_\infty^0(\tau) = 0$.

This difference is easily traced to the fact that the RPA is consistent only in the high energy, weak disorder limit. Indeed, if we explicitly take the high energy, weak disorder limit in Eqn. (4.11), i.e., $c_g^2k^2 \to \infty$ and $\mathrm{A}^2/\mathrm{cg} \to 0$, while keeping the product $(\Delta^2/c_g)(c_g^2k^2) = 4/\alpha$ a constant, we obtain the solution as

$$P_\infty(\tau) = \frac{\alpha}{\tau^2}\exp(-\frac{\alpha}{\tau}) \tag{4.12}$$

This is exactly the Universal distribution of sojourn times obtained in Eqn. (4.5) for the case of a free electron with $c_g = \hbar k/m$. This again reconfirms the delay time distribution. We note that the approximations have to be carried out consistently

only for reasonably large group velocity c_g, which is true for energies far away from the band edges. This also suggests that the condition of weak disorder $A^2k \ll 1$ for the one parameter scaling which assumes a uniform distribution of the phase (RPA), should be modified to $\Delta^2 k/(c_g/c_\phi) \ll 1$, where c_ϕ is the phase velocity.

4.4 Strong disorder and a periodic background: Numerical results

The probability distribution of the sojourn times given by Eqn.(4.5) was derived in the limit of weak disorder and high energy when the RPA is valid. In this Section, we will numerically investigate the distributions of sojourn times for the case of strong disorder and will also compare the distributions of the sojourn times and the Wigner delay times. Further, the effect of a periodic background on the delay times will be investigated.

In order to get beyond the RPA, we will use the transfer matrix method [132] to simulate the one-dimensional random medium using the one-band tight binding Hamiltonian with diagonal disorder [133]. The Hamiltonian describing the motion of a quasiparticle on a random lattice can be written as

$$\mathcal{H} = \sum_n [\epsilon_n |n\rangle \langle n| + V(|n\rangle \langle n+1| + |n+1\rangle \langle n|)] \tag{4.13}$$

where In), ϵ_n and V denote the non-degenerate Wannier orbital at the n^{th} site, the site energy at the n^{th} site and the hopping matrix element connecting the nearest neighbours separated by a unit lattice spacing respectively. The site energies ϵ_n can be written in an equivalent form of $\epsilon_n - i\eta$, with the real part of the site energy assumed to be independent random variables uniformly distributed over the range $[-W/2, W/2]$ (unless specified otherwise) for $1 < n < N$ and zero otherwise. This is so that the chain of N sites is imbedded in an infinite lattice. The imaginary part in the site energy $(-iq)$ makes the Hamiltonian non-Hermitian and causes quasiparticles to be absorbed or amplified depending on the sign of η, which is taken to be finite and constant only across the disordered segment $1 < n < N$ and zero otherwise. Since all the energies can be scaled with respect to V, we will set V to unity without loss of generality.

The reflection (R) and the transmission(T) amplitudes can now be calculated us-

ing the transfer matrix method[132]. In order to calculate the Wigner phase delay time, the reflection (transmission) amplitude $R(E) = \sqrt{r(E)}\exp[-i\theta(E)]$ is computed at two slightly differing values of the incident wave energy E = E_0 and E = $E_0 + 6$E for a conservative chain ($\eta = 0$). The Wigner phase delay time is calculated as $\tau_w = \hbar(d\theta/dE) = \hbar[\theta(E_0 + \delta E) - \theta(E_0)]/\delta E$. Similiarly, to calculate the sojourn time by applying the imaginary potential, the reflection (or transmission) amplitude is computed at two values of the imaginary site energy ($\eta = 0$ and $\eta = \delta\eta$). Now the sojourn time is given by $\tau_s = \hbar/2(d|R|^2/d\eta) = \hbar/2[|R(E,\eta = \delta\eta)|^2 - |R(E,\eta = 0)|^2]/\delta\eta$. Typically the values of δE and $\delta\eta$ are 10^{-6} and the stability of the results have been checked to their choice within the range $10^{-5} < \delta E < 10^{-7}$. In this Section, we will deal with the delay times in a dimensionless form by'multiplying with V and set $\hbar = 1$. For the calculation of the averages and the distributions, we have typically used 10^5 configurations of the disorder. We will present results for a long sample (L $\gg$ 1, lengths much greater than a localization length).

Using the above procedure, we will investigate first the distribution of the phase of the reflected wave from a long disorder medium ($|R| \to 1$), for the cases of weak and strong disorder at different energies within the band. Then, we will turn to the distribution of the Wigner delay times and the sojourn times obtained by the 'Non-Unitary' clock for the above cases. The effects of the periodic background will be seen to have drastic effects for energies close to a band-edge.

4.4.1 The phase distribution for the reflected wave

First, we will present the results for energies well within the allowed band (E = 0, 1.0). ~~For the mid-band case ($E = 0.0$), and small disorder levels, ($W = 0.1$), we find that the phase distribution is uniform.~~ At intermediate disorder level ($W = 2.0$), the distribution is symmetric about $\theta = \pi$ and two peaks are present. For higher disorder, the peaks move closer and in the limit of very large disorder, the two peaks would eventually merge into a single 6 peak [134]. This reconfirms the distributions obtained earlier by other workers [134, 135]. For the general case E = 1, we note similiar features, though the distributions have an asymmetry about $\theta = \pi$. The distributions are shown in Fig. 4.3. Now for the case of the wave energy close to the band edge (E = 1.9, 1.99), and small disorder (W = 0.1), we again find a uniform

For energies near the middele of the band (E=0.1) & small disorder levels, we find that the phase distribution is uniform. It should be noted that at exactly E=0, the phase randomization legnth diverges due to certain anamolies [135] & a uniform phase distribution is never obtained for finite lengths.

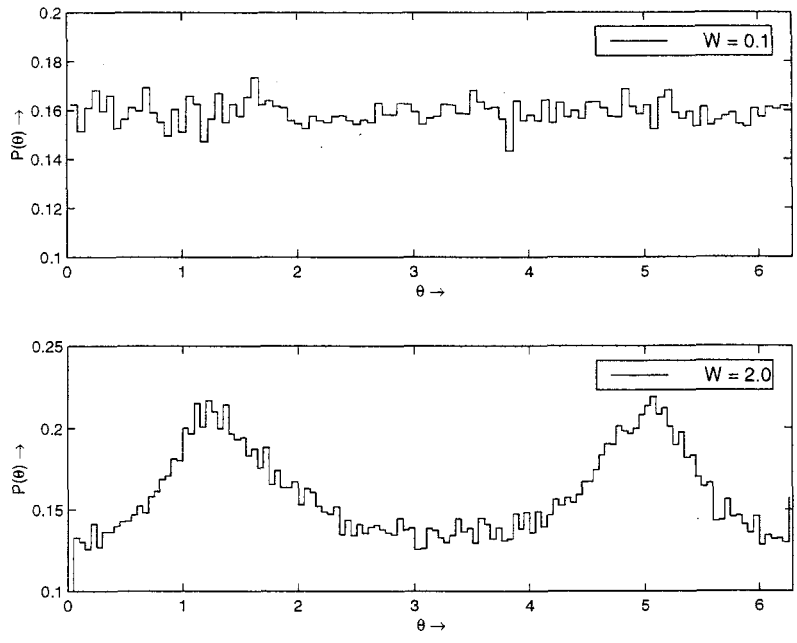

Figure 4.3: The phase distribution for reflection from a long disordered passive medium for wave energy near the middle of the band (E = 0.1).

phase distribution. For the case of strong disorder. we note a highly non-uniform distribution as before, with two peaks (Fig. 4.4). The peaks are, however. highly unequal with the asymmetry increasing with closeness to the band edge. It should be noted that in a continuum disorder model, an asymmetric distribution always results because onlv positive, non-zero energy solutions are possible. Within this one-band model, we note that the distribution of the phase reflects about $0 = \pi$. as we go over to the negative E. as can be seen from Fig. 4.4c.

In passing, we observe that if the disorder is made asymmetric about zero with the same range (W), for example, between $[0, W]$, the uniform distribution of the phase does not result even for weak disorder $(W = 0.1)$. We plot the obtained distributions in Fig. 4.5, which can be seen to be quite asymmetric about $0 = \pi$. This effect is most manifest for energies close to the bandedge. as can be seen in Fig. 4.5. The distribution has a single maximum. which tends to occur at $0 = \pi$ at energies close to the band-edge. This results from the prompt part of the reflection arising from the mismatch in the potential at the boundaries. For strong disorder. again the phase distribution is not symmetric about $0 = \pi$ for $E = 0$. There is still only one prak.

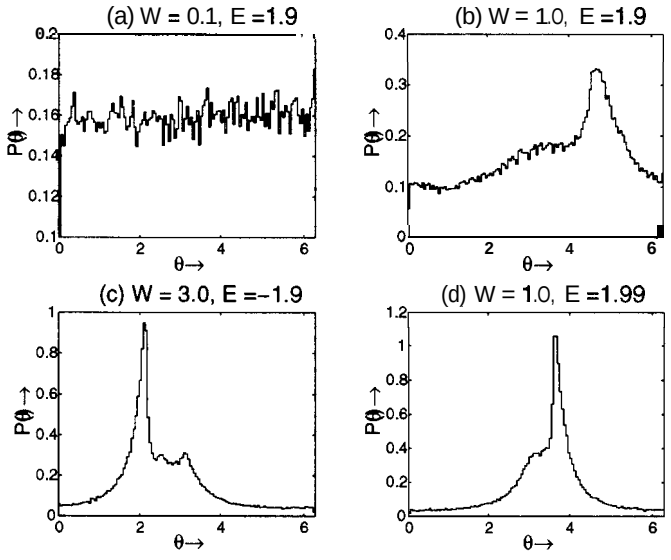

Figure 4.4: The phase distribution for from a long disordered passive medium for wave energy at the edge of the band (E= 1.9, 1.99).

This behaviour just reflects about $\theta = \pi$ if the one-sided disorder is made negative, i.e., between [−W,0] as can be seen from Fig. 4.5b.

4.4.2 Distribution of delay and sojourn times

Now, we will turn to the distribution of the delay times for reflection from the random sample. We will, first, examine the case of wave energies far away from a band edge (E= *0.0,* 1.0). In Fig. 4.6, we show the distribution of the Wigner phase delay time τ_w and the sojourn time τ_s for reflection from a long sample for different values of the disorder strengths (W = 0.1, 2). For weak disorder (W = 0.1), the distributions are identical to each other and also correspond exactly to the universal distribution given by Eqn.(4.5). The two distributions also coincide for higher disorder strengths.[2] We also note that Eqn.(4.5) still describes the distribution reasonably well for strong disorder (W = 2.0, see Fig. 4.6b), though the RPA under which the expression was derived is not valid for these cases. The case of E = 1 shows similiar behaviour, though the peak occurs at a different value, reflecting the smaller group velocity. In Fig. 4.6d, we plot the distributions of sojourn and delay times for cases of symmetric disorder ($[-W/2, W/2]$) and asymmetric disorder ([0,W] and $[-W,0]$). The distri-

[2]Note that though the two distributions over the ensemble might coincide, the phase delay time and the sojourn time for a given configuration need not be equal and, in fact, are not equal.

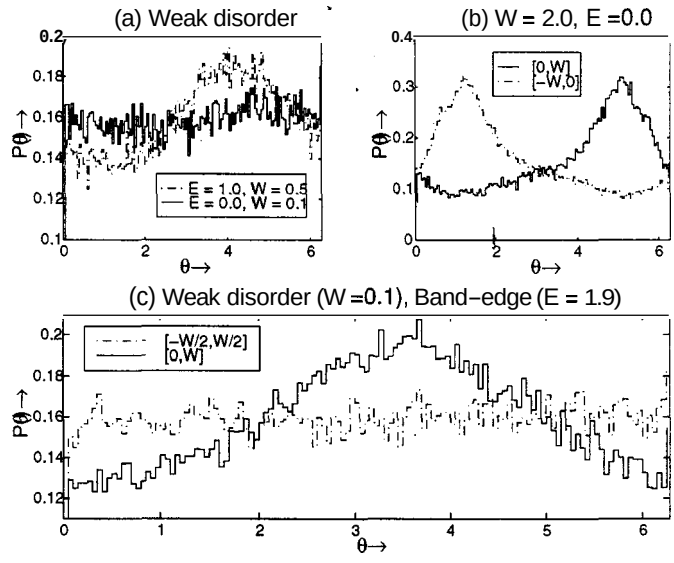

Figure 4.5: The phase distribution for from a long disordered passive medium for wave energy at the middle of the band $(E = 0.0)$ and asymmetric disorder.

butions for the positive and negative one-sided, asymmetric disorder appear to be the same, regardless of the sign. These, however, are different from the distribution for the symmetric case. The contribution of the prompt part of the reflection arising from the average potential mismatch at the boundary is clearly seen for the cases of asymmetric disorder, in that, the peak of the disorder occurs slightly earlier and there is more weight at early times.

Now, we will examine the case of wave energies close to the edge of the band $(E = 1.9,\ 1.99)$. In Fig. 4.7, we show distributions of the delay time and sojourn times. For the case of weak disorder, again the Wigner delay time distribution and the sojourn time distribution coincide. There is, however, considerable discrepancy from Eqn.(4.5), as can be seen. We know that the RPA is valid for this case, as can be seen form the distribution of the phase in Fig. 4.4. Thus, the discrepancy cannot be an artifact of the RPA.

The most probable reason is due to the reduced density of states near the band-edge and the wave never completely samples the randomness before getting reflected. Thus, the factorization of the joint distribution into the phase distribution and the delay time distribution separately becomes suspect.

For intermediate and strong disorder $(W = 1,\ 2,\ 3)$, a more interesting effect occurs. The two distributions, i.e., the Wigner delay time distribution

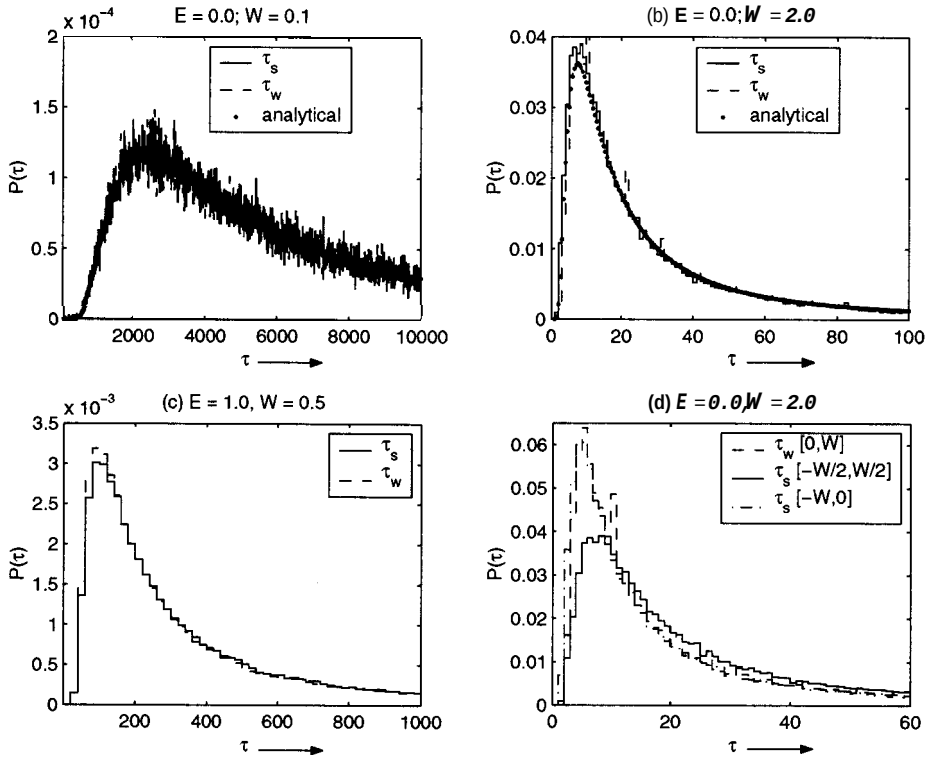

Figure 4.6: The distribution delay and sojourn times for reflection from a long disordered passive medium for wave energy at the middle of the band (E = 0.0, 1.0).

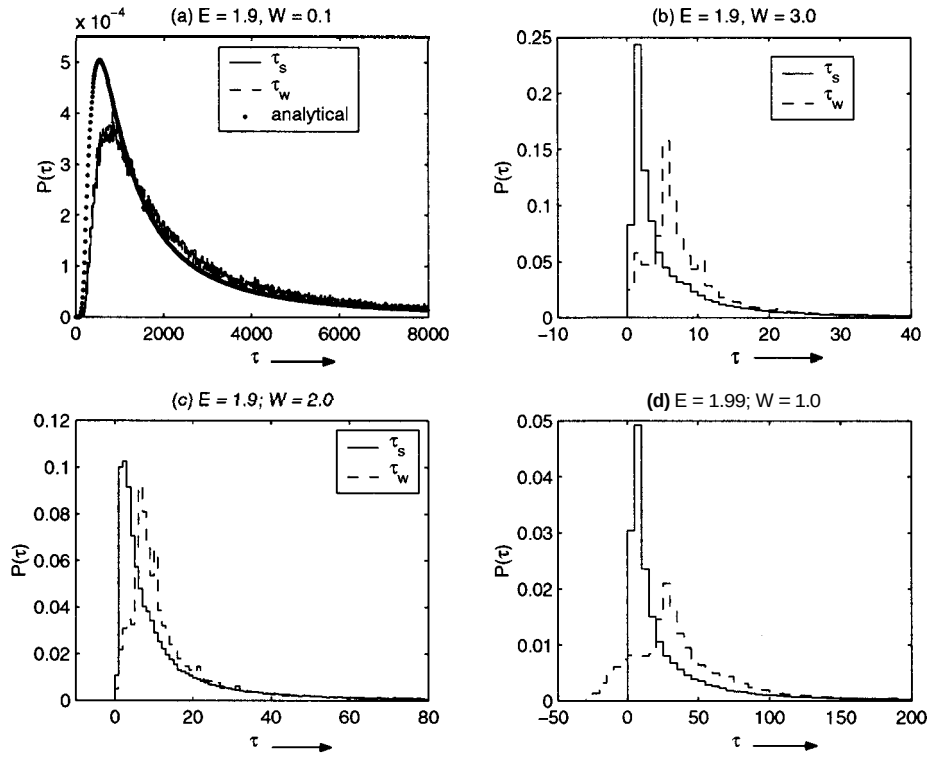

Figure 4.7: The distribution delay and sojourn times for reflection from a long dis ordered passive medium for wave energy close to the edge of the band $(E = 1.9, 1.99)$.

and the sojourn time distributions no longer coincide. The differences between the distributions increase with disorder strength and closeness to the band-edge. The Wigner delay time distribution appears quite different from the universal distribution at $E = 0$. In fact, for $E = 1.99$ and $W = 1$, the Wigner delay time distribution is non-zero for even negative times. This is, of course, due to the strong deformation of the wavepacket caused by the strong dispersion near the band-edge. The sojourn time distribution given by the 'non-Unitary' clock remains non-zero only for positive times (even though the 'spurious' scatterings have not been corrected for). We also note that the Universal τ^{-2} tail at long times $(r \to \infty)$ remains unaffected.

4.5 Conclusions

In conclusion, we have studied the distribution of the delay and sojourn times for reflection from a disordered medium. To this end, we have introduced a spatially

uniform imaginary potential as a literal counter for the time of sojourn in the sample successfully to derive the distribution of sojourn times in terms of that of the reflection coefficient. The distribution of the sojourn times derived by us for a passive medium coincides exactly with the distribution of Wigner delay times for reflection derived by Texier and Comtet [116]. The distribution appears to be universal to one-dimensional disordered systems, i.e., independent of the nature of disorder (also see [116, 120]) and is amply supported by numerical solutions. The distribution has also been recently confirmed analytically for discrete disordered systems described by a tight binding model by Ossipov *et* al. [122]. Our technique further allows us to treat the important case of an active random medium with amplification/absorption. All the moments in that case work out to be finite, This technique has also been used by other workers, in particular Beenakker *et al.*[107], to calculate the distribution of eigenvalues for transmission in the multimode case and the amplitude correlator. Beenakker has called it a mapping from the static case of an absorptive system to the dynamic case of a non-absorptive system.

We have also revisited the original calculation of Jayannavar *et al.*[117], of the distribution of the Wigner delay time. We show by explicitly taking the high-energy limit in addition to the RPA that the same universal distribution of delay times results. In the course of the derivation, we note that the single parameter scaling ansatz for the RPA seems consistent under the condition $\Delta^2 k/(c_g/c_\phi) \ll 1$ (Δ^2- the disorder strength, c_g -the group velocity and c_ϕ -the phase velocity) instead of $A^2k \ll 1$ which does not account for the effects of the group velocity. This is in accord with the recent results of Ref. [136, 122]. We have also investigated the distribution of delay times numerically and find the distributions of the Wigner delay time and the sojourn time to coincide for energies far away from a band-edge for all disorder strengths. This, however, breaks down for energies close to the band-edge and strong disorder, when the dispersive effects of the band structure deform the wavepacket so much as to render the description of the motion of a wavepacket meaningless. Under such circumstances, the concept of a sojourn time clocked by a counter such as the imaginary potential appears more meaningful.

Finally, we turn to the universality aspects of the distributions. We note that Eqn.(4.5)for the sojourn time/delay time appears universal for several models of

disorder for a one-dimensional disordered system under the assumptions of weak disorder/high energies. This has been obtained analytically for several models of disorder [116, 106, 122, 119] and also numerically [120, 116]. We also note that at high energies, the phase delay time and sojourn time almost become equal. The universal τ^{-2} tail at long times is thought to arise due to configurations with resonant transmission (Azbel resonances). This behaviour is not obtained for a chaotic cavity connected to a reservoir by a single open cavity [125]. This is presumably because the localization picture may not hold in this case. This suggests that the problems of the one-dimensional disordered systems and the chaotic cavity belong to different universality classes.

Chapter 5

Adapting the Ornstein-Uhlenbeck process to describe photon migration

5.1 Introduction

In Section 1.3.3, we described the inadequecy of the diffusion approximation when applied to the photon migration problem. The main lacuna of the diffusion approximation is that it neither accounts for a finite mean free path nor a finite speed of the diffusing particle. Thus, it fails to describe the persistence in the phase space. Therefore, it is important to investigate stochastic processes which preserve these essential features of light transport in random media. In this Chapter, we examine the application one of the earliest stochastic processes with persistence, *viz.* the Ornstein-Uhlenbeck (O-U) process of Brownian motion[137] to photon migration.

As will be seen, though the Ornstein Uhlenbeck process accounts for a finite mean free path of the particle, it makes the assumption of a distribution of speeds for the particle with a well defined mean speed. We will call this kind of a *global constraint* of a finite speed as the *"weak constraint of fixed speed"*, where the speed of the diffusing particle is allowed to fluctuate about a fixed mean. In this context, a Feynman path integral formalism has been developed recently [138], where it was attempted to describe these photon random walks with fixed speed. But the attempt was only partially successful in that, the constraint of fixed speed could only be applied in the above global weak average sense. More recently, an explicit derivation of the Feyman path integral representation of the propagator for the radiative transfer equation has

been given [139]. Here it was again evaluated by truncating the cumulant expansion after the second order which basically amounts to fixing the speed constraint in the mean while allowing Gaussian fluctuations about the mean. For comparision, we will first very briefly review this path-integral approach of Perelman et *al.*[138] in Section 5.1.1. Then, we will demonstrate that the constraint of fixed speed is relatively stronger in the O-U process by writing down the path integral for the O-U process. We also present approximate solutions for absorbing boundaries and compare the predictions with Monte-Carlo solutions of the photon random walk. We find the O-U process to be an approximate, but a more useful and accurate alternative to the diffusion approximation.

5.1.1 The path integral approach to photon migration

The path integral approach is based on the original work of Feynman (see Feynman and Hibbs[140]), where the path integral was used to deal with the randomly accelerated classical motion in the transverse direction of a high energy particle going through a medium. The path integral finds a direct application in such problems of probability due to the ease and natural ability of the path integral to deal with the notion of a sample path and the probability associated with it. In our problem of the photon (particle picture) moving around randomly in a stochastic medium, a photon can propagate between two points in space ($\vec{r_1}$ at time t_1 and $\vec{r_2}$ at time t_2) through several trajectories in the phase space. A few such possible paths in real space are shown in Fig. 5.1. With each one of these photon trajectories is associated a particular probability. this probability summed over all the possible trajectories yields the total probability for the photon to propagate between points $\vec{r_1}$ to $\vec{r_2}$. This is precisely what the path integral formalism accomplishes. In this sense the path integral approach is closest to the Monte-Carlo simulation of the problem, where different paths are simulated. But one does not normally a *priori* estimate the probability of any particular path in the Monte-Carlo simulation.

The original problem considered by Feynman and Hibbs[140], was the deflection of a fast moving, high energy particle moving through a material slab. The velocity of the particle was considered to recieve small random alterations in the transverse plane due to scattering by the fixed nuclei. Because only the transverse motion is

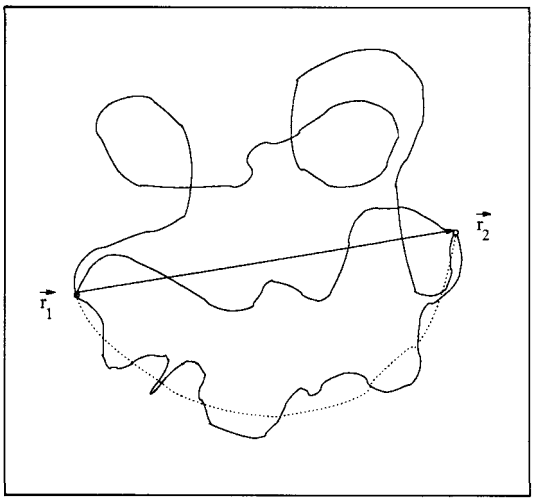

Figure 5.1: A few possible photon trajectories in real space (assumed to be two-dimensional here). The particle is at $\vec{r_1}$ at time t_1 and $\vec{r_2}$ at time t_2.

considered, the random spatial distribution of fixed scatterers traversed at a fixed longitudinal speed translates to a temporally stochastic process. Thus, it is a case of a particle randomly accelerated particle in the plane (xy-plane) perpendicular to the particle's initial velocity (along the z- axis, say). The resulting distribution shows a diffusion in the velocity space ($(x^2) \sim t$), while there is a highly non-diffusive behaviour in the real space ($(x) \sim t$ and $(x^2) \sim t^3$). This non-diffusive behaviour manifests for the quantum-mechanical case as well [141]. In this case, we have an indefinite acceleration (stochastic heating) of the particle, much as the Fermi acceleration of cosmic-ray particles to ultra-relativistic energies by interaction with various plasma modes during collisions with galactic clouds in motion[142]. Though this model of a randomly accelerated particle accounts for a finite mean free path, it is clearly inapplicable to the photon migration problem.

In the attempt of Perelman et al.[138] to impose the constant speed of light using the path integral formulation, the photon was again considered to be a randomly accelerated particle, but with the constraint of fixed speed. Taking the random deflections to have a white-noise distribution, the probability for a photon to propagate between the points $(\vec{r_1}, t = 0)$ and $(\vec{r_2}, t = T)$ can be written as an integral over all paths:

$$P(\vec{r_2}, T; \vec{r_1}, 0) = P_0 \int \mathcal{D}[\vec{r}(t)] \exp\left\{ -\frac{1}{2f_0^2} \int_0^T [\ddot{\vec{r}_i}]^2 dt \right\} \times J[r(t)] \qquad (5.1)$$

where P_0 is a normalization constant, $\mathcal{D}[\vec{r}(t)]$ is the infinitesimal function space element in the domain of all the possible path functions with the boundary conditions $\vec{r}(t=0)=\vec{r_1}$ and $\vec{r}(t=\mathrm{T})=\vec{r_2}$, and $J[\vec{r}(t)]$ denotes the density of photon paths and constrains the photons to propagate at a fixed speed (the local strong constraint), and is given by $J[\vec{r}(t)]=\delta([\dot{\vec{r}}(t)]^2-c^2)$. This non-Gaussian integral is not easy to evaluate. Perelman et al. approximately evaluated the path integral by applying, instead, the weak constraint of constant speed in the form: $\int_0^T\{[\dot{\vec{r}}(t)]^2-c^2\}dt=0$, i.e., the square of the speed averaged over the path was c^2. The path integral with the weak constraint could then be evaluated by considering harmonic perturbation about the ballistic path in the case of isotropic scatterers, or about the most probable (classical) path of the randomly accelerated particle in the case of anisotropic forward scattering media. The path integral in this approximation converges by oscillation [140]. However, the absorbing boundary conditions in their work could not be implemented properly. It is to be noted that a first-order improvement on this, *i.e.*, imposition of the strong local constraint of fixed speed, at least on the most probable path, is possible. However, the resulting non-linear differential equations for the motion are not amenable to analytical solution. Finally, in these approximations, it is not clear as to what basic stochastic process the above corresponds to and what the corresponding Fokker-Planck equation in the phase space would be. Moreover, it is non-trivial to impose absorbing boundary conditions on such path integrals.

5.2 The Ornstein Uhlenbeck process and light diffusion

In this Section, we consider the Ornstein-Uhlenbeck(O-U) process[137, 143], which concerns the diffusion in phase space of a Brownian particle. In the case of the randomly accelerated particle considered earlier, there was an indefinite acceleration of the particle because of the absence of any dissipative mechanism, i.e, the particle never equilibrates with the "bath". In general, there must be at least a Doppler friction for the Brownian particle as it will experience more head-on collisions with the bath particles than from behind (More a *priori* collisions than a posteriori !! [144]). This drag on the Brownian particle of the stochastic medium may be characterized by a phenomenological friction force $(-\beta\vec{v}$, where $\vec{v}$ is the instantaneous velocity of the par-

ticle). Now, the stochastic Langevin equation(SLE) for the Brownian motion becomes $\ddot{\vec{r}}+\beta\dot{\vec{r}}=\{(t)$, where β is the friction coefficient and $\vec{f}(t)$ is assumed to be a Gaussian distributed, δ-correlated random function with a zero mean (white-noise). This results in a distribution of speeds of the Brownian particle, but with a finite mean speed. The friction coefficient β and the components of the concomitant Gaussian white noise $\vec{f}(t)$ are related as $\langle f_i(t)f_j(t+\mathrm{T})\rangle = \frac{2\beta k_B T}{m}\delta(\tau)\delta_{ij}$ (the fluctuation-dissipation theorem)so as to be consistent, in the limit $t \to \infty$, with the condition of thermal equilibrium with the thermal bath at temperature T, where k_B is the Boltzmann constant and m is the mass of the particle. The first and second moments of the velocity and displacement given by this SLE are $\langle\dot{\vec{r}}\rangle = \vec{v}_0 e^{-\beta t}$, $\langle\dot{\vec{r}}^2\rangle = \vec{v}_0^2 e^{-2\beta t} + f_0^2/(2\beta)(1-e^{-2\beta t})$, $\langle\vec{r}\rangle = \vec{r}_0 + \vec{v}_0/\beta(1-e^{-\beta t})$, $\langle\vec{r}^2\rangle = 3f_0^2/\beta^3(\beta t - 3 + 4e^{-\beta t} - e^{-2\beta t})$. We clearly see that a phase-space memory is retained for a time $t \sim t^* = \beta^{-1}$, and the process smoothly interpolates between the ballistic motion at short times ($t \ll t^*$)when (r^2) $\sim t^2$ and the diffusive limit at long times ($t \gg t^*$) when (r^2) $\sim$ t. The marginal probability distribution for the spatial position of the particle undergoing the O-U process in a unbounded medium is given by[143]:

$$P(\vec{r},t;\vec{r}_0,\vec{v}_0,0) = \left[\frac{m\beta^2}{2\pi k_B T\xi(t)}\right]^{3/2} \exp\left[-\frac{m\beta^2}{2k_B T\xi(t)}\left|\vec{r}-\vec{r}_0-\frac{\vec{v}_0}{\beta}(1-e^{-\beta t})\right|^2\right] \quad (5.2)$$

where $\xi(t) = 2\mathrm{Pt} - 3 + 4e^{-\beta t} - e^{-2\beta t}$.

5.2.1 Adapting the O-U process to light

We expect that the O-U process having phase space persistence may be able to better describe photon migration than zero-persistence diffusion. The forward scattering (anisotropic scattering) is captured by describing it as a Brownian particle with a large inertia. Further, phase space (directional) memory is retained for a time $\sim t^*$.

Of course, it is recognized that there is no thermal bath and inertia for a photon. We can, however, make the following identifications from merely kinematical considerations. We will equate the root mean squared (r.m.s.) speed as also the initial speed v_0 of the photons, to c, the speed of light in the medium, and obtain $\langle\vec{v}^2\rangle = c^2 = \frac{3k_B T}{m}$, $D = \frac{cl^*}{3} = \frac{k_B T}{m\beta}$, and $\frac{|\vec{v}_0|}{\beta} = \frac{c}{\beta} - l^*$. In terms of these, we rewrite the

propagator(5.2) in an infinite medium as

$$P_\infty(\vec{r},t;\vec{r_0},\vec{v_0},t=0)=\left[\frac{3}{2\pi l^{*2}\xi(t)}\right]^{3/2}\exp\left[-\frac{3}{2l^{*2}\xi(t)}\left|\vec{r}-\vec{r_0}-l^*\hat{n}(1-e^{-ct/l^*})\right|^2\right] \tag{5.3}$$

We note that the propagator yields the diffusive behaviour at long times. Further, note that the diffuse source is at a distance l^* from the point of injection - often a major consideration in applying the diffusion approximation to the photon migration problem[145].

5.2.2 How strong is the 'weak constraint' of fixed speed in the O-U process ?

As noted before, the O-U process results in a distribution of speeds about a fixed r.m.s. speed (taken to be c by us), implying thus the weak constraint of constant speed. The question is, how strong is this weak constraint now effectively imposed by the fluctuation-dissipation theorem?

Let us write down the corresponding path integral for the O-U process in our usual notation:

$$P(\vec{r},\vec{v},t;\vec{r_0},\vec{v_0},0)=P_0\int\mathcal{D}[\vec{r}(t)]\exp\left\{-\frac{1}{2f_0^2}\int_0^T dt\ [\ddot{\vec{r}}(t)+\beta\dot{\vec{r}}(t)]^2\right\}, \tag{5.4}$$

where $\mathcal{D}[\vec{r}(t)]$ is the infinitesimal function space element in the domain of all the possible path functions with the appropriate boundary conditions(i.e., linking the point of injection and the point of detection or of exit). This path integral is Gaussian and can be exactly evaluated. We notice that the path integral converges by exponential damping for paths far away from the classical path. Thus we conclude that the global constraint on the mean speed imposed by the fluctuation-dissipation theorem is a much stronger constraint than the weak average constraint considered earlier by Perelman et al. [138] in the form $\int_0^{\cdot}\left(\dot{\vec{r}}^2-c^2\right)dt=0$, where the path integral converges by oscillation.

5.2.3 Comparision between the O-U process and the diffusion approximation

The diffusion approximation is a Wiener process for the spatial position of the photon with no directional persistence while the O-U process is more physical and describes

diffusion in the phase-space. Thus we have $\langle \vec{r}^2 \rangle \sim$ t for all times in the diffusion approximation, which is unphysically super ballistic for short times (t $\ll$ t*). On the other hand, the O-U process smoothly interpolates between a ballistic regime at short times (t $\ll$ t*) when $\langle \vec{r}^2 \rangle \sim t^2$ and diffusion at long times($t \gg$ t*)when $\langle \vec{r}^2 \rangle \sim$ t. Thus the O-U process captures the ballistic aspect of transport at short times where diffusion utterly fails (It should be noted that the propagator is Gaussian in both cases). In the case of diffusion approximation, where ($l^* \to 0$), this arises because of the unphysical infinite (unbounded) speed inbuilt into it. In the case of the O-U process, this arises due to the Gaussian tail in the velocity distribution upto infinite velocities, even though the r.m.s speed is finite and fixed. One notes that, in the diffusion approximation, the 'diffuse' (isotropic) source is taken to be at a point about a mean free path away from the point of injection, in the direction of injection (i.e., at $l^*\hat{n}$). In the O-U process, this source 'moves' in time: it is at the point of injection at $t = 0$ (as it should be) and tends to $l^*\hat{n}$ at large times interpolating in between smoothly. Also note that such important 'dynamics' occurs mainly at early time comparable to the mean free time when the randomization of the direction occurs. Though, the O-U process accounts for a finite mean free path and finite average speed, it does not strictly keep the speed of light fixed and hence, it does not preserve the light front. There exists a small acausal (faster than light) Gaussian tail due to the distribution of speeds.

5.2.4 Approximate solution to the O-U process in the presence of absorbing boundaries

An absorbing boundary means that when the particle arrives at the boundary, it becomes incapable of further motion (quenched), or it is removed immediately (absorbed). Consider an absorbing boundary along the $z = 0$ plane, with the stochastic medium occupying the negative half space (see Fig. 5.2). For the case of pure diffusion, the absorbing boundary condition corresponds to requiring the probability density at the absorbing boundary to vanish, *i.e.*, $P(x, \mathrm{y}, z = 0; \mathrm{t}) = 0$[143]. This condition, however, was found to be inadequate to describe most transport processes due to the non-Markovian nature. Recognizing the existence of a mean free path and a finite speed of propagation, the net particle flux given by Fick's law can be broken up into an outward(J_+) and inward (J_-) partial component, normal to the boundary.

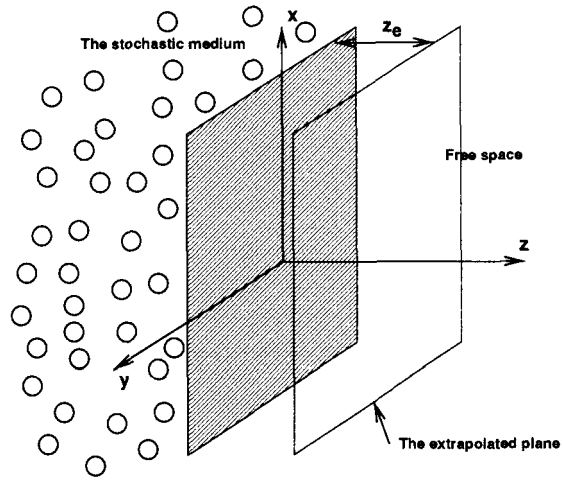

Figure 5.2: Schematic diagram showing the absorbing boundary at the $z = z_0$ plane and the extrapolated boundary plane at $z = z_e$ plane. The stochastic medium occupies the negative half-space

The absorbing boundary condition is then interpreted as that the incoming partial flux $(J_-|_{z=0})$ is zero. Expanding the diffuse energy density near the boundary to the first order in a Taylor expansion, one gets the boundary condition for the absorbing boundary as

$$J_-|_{z=o} \simeq P(x, y, z = 0, t) + 2/3\ l^* \frac{\partial P(x, y, z, t)}{\partial z}|_{z=0} = 0. \tag{5.5}$$

The effect of a (diffuse) finite boundary reflectivity (R) arising due to the average change in the refractive index at the boundary can easily be incorporated by noting that $J_- = RJ_+$ at the boundary. One can further approximate the derivative to linear order as

$$\frac{\partial P(x, y, z, t)}{\partial z}|_{z=0} \simeq \frac{P(z_e) - P(z = 0)}{z_e}, \tag{5.6}$$

i.e., we linearly extrapolate the behaviour at the boundary to the region outside the boundary and apply the absorbing boundary $P(x, \mathrm{y}, z_e, \mathrm{t}) = 0$ at an extrapolated length (z_e) outside the boundary. The value of the extrapolation length z_e is about $2/3$ [146, 147]. Note that for pure diffusion $(l^* \to 0)$, all these conditions reduce to $P(x, \mathrm{y}, z = 0, \mathrm{t}) = 0$.

For the O-U process, the absorbing boundary condition at the $z = 0$ plane has to be implemented in the phase space as:

$$P(\vec{r}', \vec{v}, t; \vec{r}_0, \vec{v}_0, 0) = 0 \quad \textit{for}\ \mathrm{v},\ < 0, \tag{5.7}$$

where $\vec{r}' = (x, y, 0)$, i.e, there are no incoming particles. The boundary condition is applied along the negative half line for the z component of the velocity. This problem was unsolved for a long time since 1945, when Uhlenbeck and Wang[148] proposed it. It was not even clear whether the problem posed as such had a unique solution. It was solved only in 1985 by Marshall and Watson[149] for a semi-infinite half-space with a single absorbing boundary by expanding for the solution in a complete set of functions which span the space with $v_z > 0$ at the boundary. However, the solutions are not in closed form and it has only been possible to evaluate asymptotic properties such as the persistence exponent [150] and the first passage time [149].

Here, we propose the following approximate solution for a single absorbing boundary at $z = 0$. We use the method of mirror images which is exact for pure diffusion. The probability distribution function in the semi-infinite half space for $x < 0$ is is given approximately by

$$P_b(\vec{r}, t; z_0\hat{z}, c\hat{z}, 0) = P_\infty(\vec{r}, t; z_0\hat{z}, c\hat{z}, 0) - P_\infty(\vec{r}, t; z'\hat{z}, -c\hat{z}, 0) \tag{5.8}$$

where $x' = -z_0$ is the position of the (negative) image source. In the diffusion approximation, one imposes the absorbing boundary conditions not at the physical boundaries but at extrapolated boundaries at a distance $z_e = 2l^*/3$ outside the slab [146]. At times long compared to the 'randomization time' ($t > t^*$), the above solution should match with the diffusion approximation. However, for short times ($t \sim t^*$), the photons are ballistic and traverse only the true thickness of the medium. In the absence of a comprehensive theory for the boundary position, we adopt the following interpolation scheme. The extrapolated boundary is kept at the physical boundary at short times upto $t = t^*$ after which it is smoothly moved to z_e outside the physical boundary asymptotically as $t \to \infty$, giving the image source position as

$$z' = -z_0 - \theta(t - t^*)\{1 - \exp[-(t/t^* - 1)]\}z_e, \tag{5.9}$$

where θ is the Heaviside step function. It should be noted that a fitting parameter of the order of unity could have been used to determine the time at which the boundary starts to move. However, only a qualitative understanding is being attempted and such a parameter is unnecessary.

The above analysis can be readily extended to a finite slab of thickness L (and of infinite extent along x and y directions). We can write the probability distribution

function for the photon density as

$$P_L(\vec{r},t;\vec{r_0},\vec{u_0},t=0) = \sum_{n=-\infty}^{+\infty} [P_\infty(\vec{r}+2nL_{eff}\hat{z},t;z_0\hat{z},c\hat{z},t=0) - P_\infty(\vec{r}+2nL_{eff}\hat{z},t;-z_0\hat{z},-c\hat{z},t=0)], \quad (5.10)$$

where L_{eff}, the effective slab thickness is obtained by the same extrapolation scheme as

$$L_{eff} = \mathrm{L} + 2\theta(t-\mathrm{t}^*)\{1-\exp[-(t/t^*-1)]\}\, z_e. \quad (5.11)$$

This solution for absorbing boundaries holds only approximately in the limits which we explain below. The equation for the marginal probability distribution for the position does not remain invariant when the initial velocity $\vec{v_0}$ and the initial position $\vec{r_0}$ are changed. In the O-U process, paths retain for a time t*, due to inertia, a 'memory' of their initial direction. Thus, at times short compared to the randomization time t*, or when the distance between the source and the absorbing boundary is less than the transport mean free path, the method of images is not strictly valid as there is an imperfect cancellation of forbidden photon paths and their mirror images. This error, however, decreases exponentially with increasing slab thickness and with increasing time. Also, as can be seen in our results, the errors are small enough to be neglected for the thicknesses we have considered ($\mathrm{L} \geq l^*$) with the source located at the centre of the slab. The series (5.10) is absolutely and uniformly convergent. The normalization $\int P_L(\vec{r},t;\vec{r_0},\vec{u_0},t=0)d^3r$ decays with time, corresponding to the flux of probability density which leaks out of the slab.

Now, we will compare the above approximate solutions for the O-U process with Monte-Carlo solutions obtained for the photon migration problem. The details of the Monte-Carlo simulations can be found in[151]. Fig. 5.3(a) shows graphically the effect of the various boundary conditions. The circles represent the number of photons in the slab as a function of time, normalized to 1, obtained from Monte Carlo simulations for a slab thickness of $\mathrm{L} = 21^*$ for nearly isotropic scatterers with $g = 0.06$. The curve marked 'a' shows the result when the extrapolated boundaries are maintained at the physical boundaries of the cell. As can be seen, while this curve approximately captures the time at which photons begin to escape from the cell and the photon number density begins to reduce, it completely fails to fit the long time diffuse tail. The curve marked 'b', is one in which the extrapolated boundaries are

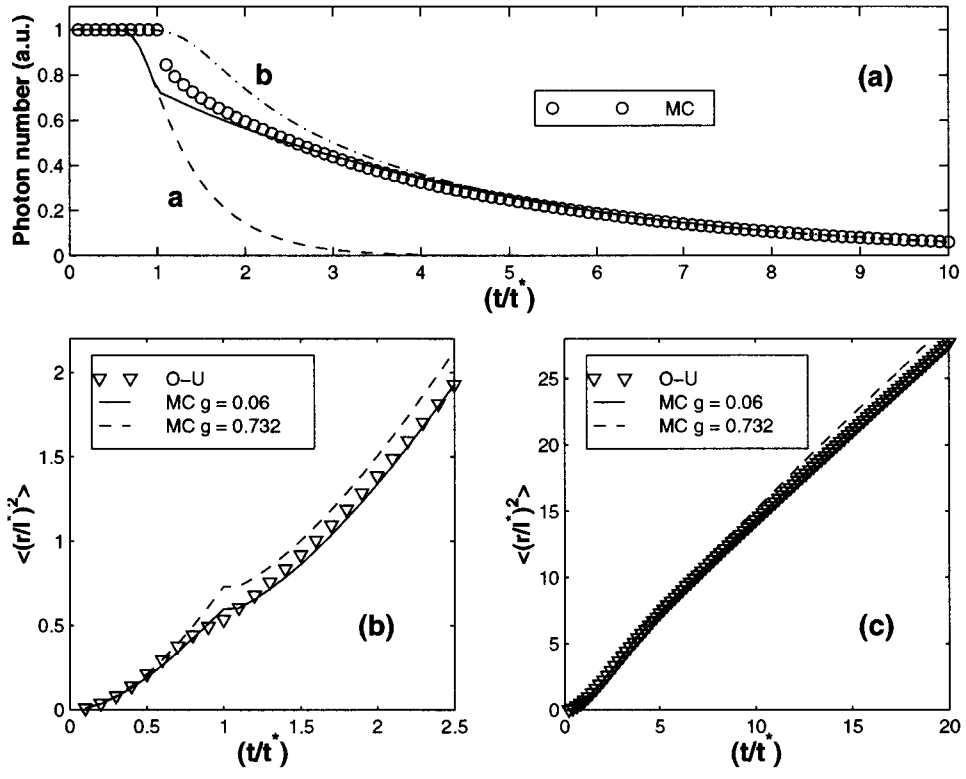

Figure **5.3:** Comparison of results obtained by modelling photon transport using the Ornstein-Uhlenbeck process with those obtained from random walk simulations. Fig.(a) compares the rate at which photons exit the slab when different boundary conditions are applied. The lower figures compare the mean square displacement calculated by integrating equation (5.10) with the random walk simulations for different slab thicknesse s. Fig.(b) shows a thin slab where the diffusion approximation is not valid while Fig.(c) is for a slab where the transport is mainly diffusive.

held at the extrapolation length $z_e = 2l^*/3$ throughout. There is excellent agreement at long times with the Monte Carlo data but the pulse exits the medium much later than the ballistic pulse, a consequence of the ballistic pulse having to traverse a medium whose thickness is $L+2z_e$. The solid line is the result of our moving boundary conditions which fits curve 'a' almost exactly at short times and agrees very well with the Monte Carlo data at long times. It is to be noted though that even when the extrapolation length is set to zero, the ballistic pulse exits the slab faster than a true ballistic pulse would do. This is a consequence of the fact that we model the photons as having a distribution of speeds. As a result, there are photons that are travelling with a speed greater than the speed of light in the medium resulting in this artefact of 'pre-ballistic' photons. As the slab thickness is increased this effect becomes vanishingly small since there are almost no ballistic photons in the medium. However, it is important to appreciate that the OU process describes most of the essential features of the simulation at short times which would not be possible using the diffusion approximation.

Fig. 5.3(b) compares the results obtained for the mean square displacement of the photons from the point at which they are launched, as a function of time, for a cell of thickness $L = 2l^*$. At short times the transport is predominantly ballistic and the mean square displacement shows the characteristic quadratic behaviour. The kink in the curves occurs when the ballistic photons exit the slab. At this point, the fastest moving photons are lost and thus the average value of the mean square displacement is sharply lowered. The OU process compares well with the Monte Carlo data for nearly isotropic scatterers. Fig. 5.3(c) shows the same data but for a cell whose thickness $L = 8l^*$. Now the regime is one, where the diffusion approximation is valid, and excellent agreement is obtained between the OU process and Monte Carlo data for isotropic scatterers. The data for anisotropic scatterers appears to slightly deviate from that of isotropic scatterers and the O-U process. This could be due computational inaccuracy of truncation/round-off errors, as more number of computational operations are required to propagate the photons in the case of anisotropic scatterers. Thus, despite the fact that the method of images is not strictly valid for early times, we find that the OU process proves reasonably effective in capturing most of the features of photon transport in confined geometries.

5.3 Conclusions

In this chapter, we have examined some models to describe photon migration in turbid media. In particular, we have adapted the Ornstein-Uhlenbeck process of Brownian motion for this purpose. These models incorporate a finite mean free path as well as implementing the constraint of a constant speed for the photon in a weaker 'average' sense. We also reviewed the path integral approach of Perelman et *al.* to photon migration. The path integral approach suggests that the global constraint of a fixed speed in an average sense in the O-U process is much stronger than that in the earlier proposed model of Perelmen et al. Approximate solutions for the O-U process with absorbing boundaries have been given using the method of images. These solutions have been compared with the diffusion approximation and Monte-Carlo solutions. They offer a reasonable solution in the intermediate scattering regime ($l^* < \mathrm{L} < 8L^*$) between ballistic motion on one hand and diffusive trasport on the other. In view of the simplicity of the expressions, they should be a useful approximation.